ISSN 1068-3356, Bulletin of the Lebedev Physics Institute, 2017, Vol. 44, No. 7, pp. 198–201. © Allerton Press, Inc., 2017.
Original Russian Text © V.I. Mazhukin, O.N. Koroleva, A.V. Mazhukin, Yu.A. Aleshchenko, 2017, published in Kratkie Soobshcheniya po Fizike, 2017, Vol. 44, No. 7, pp. 20–26.

Effect of Degenerate Carriers on Si Band Gap Narrowing

V. I. Mazhukin[a,b], O. N. Koroleva[a,b], A. V. Mazhukin[a,b], and Yu. A. Aleshchenko[b,c]

[a] *Keldysh Institute of Applied Mathematics, Russian Academy of Sciences, Miusskaya pl. 4, Moscow, 125047 Russia; e-mail: vim@modhef.ru*
[b] *National Research Nuclear University "MEPhI", Kashirskoe sh. 31, Moscow, 115409 Russia*
[c] *Lebedev Physical Institute, Russian Academy of Sciences, Leninskii pr. 53, Moscow, 119991 Russia*

Received May 4, 2017

Abstract—Various mechanisms causing band gap narrowing in strongly heated silicon are considered. In the high-temperature region, it becomes necessary to use Fermi–Dirac quantum statistics to describe carriers, since the silicon chemical potential appears in the valence band and in the conduction band at high carrier concentrations. It is shown that carrier degeneracy under conditions of sufficiently strong heating of intrinsic semiconductor causes strong band gap narrowing. The obtained values of band gap narrowing are compared to experimental results.

DOI: 10.3103/S106833561707003X

Keywords: silicon, carrier concentration, quantum and classical statistics, band gap narrowing.

Pulsed laser exposure of silicon is a region of active fundamental [1] and applied [2] studies for many years. In this context, much attention is paid to the problem of determining the properties of this semiconductor and its plasma in a wide range of parameter variations, i.e., the temperature, pressure, and the intensity, duration and wavelength of the laser radiation. For example, the exposure to nanosecond and picosecond laser pulses in due time caused an acute discussion about melting mechanisms [3] and properties of high-density electron-hole plasma [4]. These studies are urgent at the present time as well. Extensive experimental and theoretical data allowed the conclusion [5] that silicon relates to semiconductors in which covalent bonds are broken during melting with a change in the short-range order and a sharp increase in the conduction electron density, resulting in the silicon transition to the metal state. However, the role and effect of one of the most important silicon characteristics, i.e., the band gap E_g in the high-temperature region remained unrevealed both experimentally and theoretically.

The capability of optical experiments [4] and experiments based on photoluminescence spectroscopy [6] is very limited in the melting region. The theoretical approaches in the high-temperature region $T \approx T_m$, where T_m is the equilibrium melting temperature, and above face the circumstance that the carrier concentrations N_e, N_h in this temperature region reach $N_e \approx 10^{18}$ cm^{-3} and above. To describe the carrier states at such densities, it becomes necessary to use quantum statistics, i.e., the Fermi–Dirac (F–D) distribution function and integrals.

The objective of this work is to study the behavior of the fundamental silicon characteristic, i.e., the band gaps and its variation under conditions of thermodynamic equilibrium with increasing temperature and carrier concentration. Special attention is paid to the determination of the most important semiconductor characteristic, i.e., the equilibrium carrier concentration in the melting region.

In the simplest cases, i.e., for intrinsic semiconductors ($N_e = N_h$) under conditions of thermodynamic equilibrium in the low-temperature region $T \approx 300$ K, the determination of the temperature dependences of electron $N_e(T)$ and hole $N_h(T)$ densities is not a serious problem, since carriers are non-degenerate and obey the Maxwell–Boltzmann (M–B) statistics [7],

$$N_e(T) = N_h(T) = N_i(T) = \frac{1}{2}\left(\frac{2k_BT}{\pi\hbar^2}\right)^{3/2} M^{1/2}(m_e m_h)^{3/4} \exp\left(-\frac{E_g}{2k_BT}\right), \qquad (1)$$

where m_e, m_h are the effective mass tensors for the conduction band and the valence band, k_B is the Boltzmann constant, $\hbar$ is the Planck constant, M is the number of valleys in the conduction band, for silicon, $M = 6$.

The semiconductor is non-degenerate until the conditions

$$E_C - \mu \gg k_B T, \;\; \mu - E_V \gg k_B T \tag{2}$$

are satisfied for it, where μ is the chemical potential (Fermi level), E_C is the lower boundary of the conduction band, and E_V is the top of the valence band.

The determination of intrinsic concentrations in silicon is significantly complicated in the high-temperature region $T \leq T_m$. The quantities E_g, μ and $N_e(T)$ become interdependent. Due to the high carrier concentrations, the chemical potential approaches the top of the valence band. Non-degeneracy conditions (2) are not satisfied, M–B statistics becomes invalid, and expression becomes inapplicable. In this case, the electron and hole states should be described using F–D quantum statistics; the concentrations should be determined using F–D integrals of the order of $k = 1/2$: $\mathcal{F}_{1/2}(\eta_e)$ and $\mathcal{F}_{1/2}(\eta_h)$,

$$N_e(T) = N_C \mathcal{F}_{1/2}(\eta_e), \;\; N_C = 2M(m_e k_B T/2\pi\hbar^2)^{3/2},$$

$$\mathcal{F}_{1/2}(\eta_e) = 1/\Gamma(3/2) \int\limits_0^\infty \varepsilon^{1/2}/1 + \exp(\varepsilon - \eta_e) d\varepsilon,$$

$$N_h(T) = N_V \mathcal{F}_{1/2}(\eta_h), \;\; N_V = 2M(m_h k_B T/2\pi\hbar^2)^{3/2}, \tag{3}$$

$$\mathcal{F}_{1/2}(\eta_h) = 1/\Gamma(3/2) \int\limits_0^\infty \varepsilon^{1/2}/1 + \exp(\varepsilon - \eta_h) d\varepsilon,$$

where $\eta_e = -(E_C - \mu)/k_B T, \;\; \eta_h = -(\mu - E_V)/k_B T$ is the reduced chemical potential, N_C, N_V are the electron and hole densities of states, respectively.

To calculate the F–D integrals of integer and half-integer orders, the convenient approximation was proposed in [8, 9], according to which the integrals of order $k = 1/2$ are presented in the form

$$\mathcal{F}_{1/2}(\eta_e) = \exp\left(\sum_{i=0}^{7} a_i \eta_e^i\right), \quad \mathcal{F}_{1/2}(\eta_h) = \exp\left(\sum_{i=0}^{7} a_i \eta_h^i\right). \tag{4}$$

The electrical neutrality condition with regard to the approximation (4) takes the form

$$N_e(T) - N_h(T) = N_C \exp\left(\sum_{i=0}^{7} a_i \eta_e^i\right) - N_V \exp\left(\sum_{i=0}^{7} a_i \eta_h^i\right) = 0. \tag{5}$$

In this case, the band gap intricately depends on the lattice temperature T and carrier concentration N_e [10] and exhibits significant narrowing due to the convergence of the boundaries of the bottom of the conduction band with the top of the valence band. Three main mechanisms cause the band gap narrowing effect: lattice thermal expansion, electron-lattice interaction, and collective interactions of carriers. The thermal expansion with increasing temperature, along with the electron-lattice interaction enhancement, causes a displacement of relative position of the conduction and valence bands. In the low-temperature region $T \leq 300$ K, the thermal effect is nonlinear in contrast to higher temperatures where the temperature dependence of the band gap variation is linear. The total manifestation of the first two band gap narrowing mechanisms is described by the semi-empirical dependence [11]

$$E_g(T, N_e) = E_{g,0} - \alpha T^2/(T + \beta), \tag{6}$$

where $E_{g,0} = 1.169$ eV is the band gap at a temperature of 0 K, α and β are the constants whose experimental estimates for silicon are $\alpha = 7.021 \cdot 10^{-4}$ eV/T and $\beta = 1108$ K.

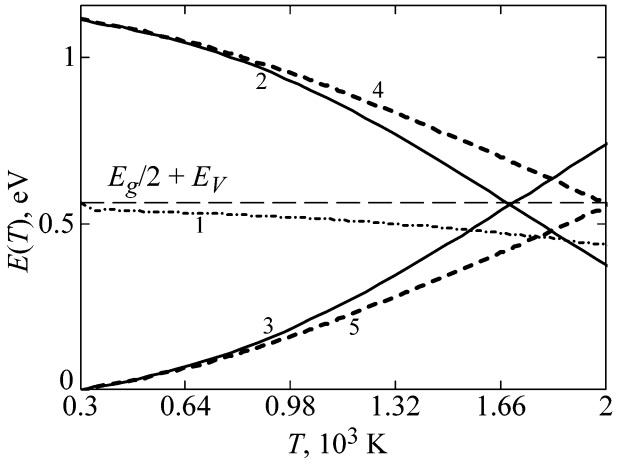

Fig. 1

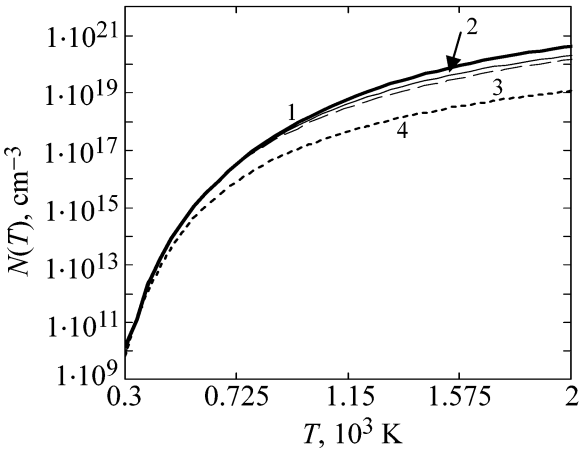

Fig. 2

Fig. 1. Temperature dependences (1) $\mu(T)$; $E_C(T)$ and $E_V(T)$ with parameters: (2), (3) $\gamma = 8.35 \cdot 10^{-8}$ eV·cm; (4), (5) $\gamma = 4.2 \cdot 10^{-8}$ eV·cm.

Fig. 2. Temperature dependences $N_e(T)$. Statistics: F–D (1) $\gamma = 8.35 \cdot 10^{-8}$ eV·cm, (2) $\gamma = 4.2 \cdot 10^{-8}$ eV·cm; M–B (3) taking into account the temperature dependence of E_g, (4) $E_g = \text{const} = 1.12$ eV.

The third band gap narrowing mechanism is associated with the effects of the collective interactions of carriers, which become dominating at sufficiently high concentrations. The quantum effects become appreciable at carrier concentrations $N_e \approx 10^{18}$ cm^{-3} and is formulated in a complex way [12]. The most significant contribution to the band gap narrowing is made by the exchange interaction estimated by the empirical dependence of the form $\Delta E_g(N_e) \sim \gamma \cdot N^{1/3}(T)$ [13], where γ is the fitting parameter used to bring into coincidence the theoretical estimates with experimentally determined values of band gap narrowing in various semiconductors.

The Si band gap narrowing can be estimated taking into account all mechanisms at high temperatures and carrier concentrations $N \approx 10^{18}$–10^{21} cm^{-3} within the semi-empirical dependence [11]

$$E_g(T, N) = E_{g,0} - \alpha T^2/(T + \beta) - \gamma N^{1/3}(T). \tag{7}$$

The fitting parameter γ for wide band-gap semiconductors $1.1 < E_g < 3.5$ eV at temperature $T \approx 300$ K and concentration $N = 10^{17} - 10^{19}$ cm^{-3} is in the range of $(2.69 - 7.3) \cdot 10^{-8}$ eV·cm [13, 14]. For silicon, under the same conditions, the parameter γ is in the range of $(1.0 - 3.6) \cdot 10^{-8}$ eV·cm [12, 15]. In this study, the fitting parameter γ for Si was taken as parameter $\gamma = 8.35 \cdot 10^{-8}$ eV·cm for the reasons of the band gap zeroing at $T = T_m = 1687$ K.

The calculated results are shown in Figs. 1–2. Figure 1 shows the temperature dependences of the silicon chemical potential $\mu(T)$ and the conduction $E_C(T)$ and valence $E_V(T)$ band edges, which give pictorial presentations of the band gap shape and narrowing rate $E_g(T, N)$. The chemical potential calculated from Eq. (5) progressively deviates from the midgap toward the valence band $E_V(T)$ with increasing temperature. The convergence of curves $\mu(T)$ and $E_V(T)$ is defined by the ratio of the electron and hole effective masses, which is $Mm_e/m_h = 1.89$ for silicon. Beginning with $T = 1000$ K, the carrier concentration (Fig. 2) and the band gap (Fig. 1) calculated with quantum and classical statistics begin to differ: for F–D, $N_h(T) = 1.5 \cdot 10^{18}$ cm^{-3}, $E_g(T, N_h) = 0.73$ eV; for M–B, $N_h(T) = 9.1 \cdot 10^{17}$ cm^{-3}, $E_g(T) = 0.81$ eV. The data obtained correspond to weak degeneracy ($\eta_h \approx -4$).

The strong degeneracy region arises in the case of crossing $\mu(T)$ and $E_V(T)$ which corresponds to $\eta_h = 0$ and $T = 1600$ K, $N_h = 1.1 \cdot 10^{20}$ cm^{-3}, $E_g(T, N_h) = 0.083$ eV for the F–D distribution and $N_i = 3.8 \cdot 10^{19}$ cm^{-3}, $E_g(T) = 0.48$ eV for the M–B distribution.

The same pattern with a certain shift to higher temperatures is observed with electron gas degeneracy. Weak degeneracy: $\eta_e \approx -4$, $T = 1090$ K, $N_e(T) = 4.5 \cdot 10^{18}$ cm^{-3}, $E_g(T, N_e) = 0.61$ eV; strong degeneracy: $\eta_e \approx 0$, $T = 1920$ K, $E_g(T, N_e) = -0.28$ eV. For the equilibrium melting temperature $T =$

$T_m = 1687$ K in the version with quantum statistics and the fitting parameter $\gamma = 8.35 \cdot 10^{-8}$ eV·cm, the band gap vanishes $E_g(T, N_h) = 0$ with the carrier concentration $N_h(T) = 1.7 \cdot 10^{20}$ cm^{-3}. Upon further heating to $T = 2000$ K, the band gap becomes negative, and the carrier concentration continues to increase, $N_h(T) = 4.2 \cdot 10^{20}$ cm^{-3}, $E_g(T, N_h) = -0.38$ eV.

For the M–B distribution, the band gap still remains positive, and the concentration is significantly lower than that for the F–D statistics: $E_g(T) = 0.24$ eV, $N_i = 1.4 \cdot 10^{20}$ cm^{-3}. As the fitting parameter twofold decreases, $\gamma = 4.2 \cdot 10^{-8}$ eV·cm, the band gap vanishes $E_g(T, N_h) = 0$, $T = 2000$ K and $N_h(T) = 2.05 \cdot 10^{20}$ cm^{-3}. The analysis performed allowed the following conclusions:

(i) Under conditions of thermodynamic equilibrium, carrier degeneracy in silicon with intrinsic conductivity begins at a temperature significantly below the equilibrium melting temperature. This requires the use of quantum statistics and technique of calculating the F–D integrals when determining properties of solid-state silicon.

(ii) The concentrations of both carrier types indicate their strong degeneracy in the temperature range $T = 1600 - 2500$ K. The consideration of quantum effects makes it possible to zero the band gap $E_g(T, N_h) = 0$ at the equilibrium melting point or its vicinity. The concentrations are in the range $N(T) = 4.2 \cdot 10^{20} - 10^{21}$ cm^{-3} which is typical of semimetals with negative band gap [7], but is below the concentrations typical of metals by several orders of magnitude, $10^{22} \cdot 10^{23}$ cm^{-3}.

(iii) Thermodynamic equilibrium melting of undoped crystalline silicon occurs in two stages. First, the melt gains semimetal properties with the number of carriers increasing with temperature. Then, upon reaching a certain temperature $T \gg T_m$, molten silicon takes metallic properties with constant electron and hole concentrations.

(iv) The above analysis is very important to better understand nonequilibrium heating and melting of pure crystalline silicon, e.g., by ultrashort femtosecond laser pulses [1, 4]. While satisfying the condition $\hbar\omega_L > E_g(T, N)$, where $\hbar\omega_L$ is the laser radiation photon energy, electron and hole concentrations $N(T) \approx 10^{22}$ cm^{-3} can be reached in solid silicon due to photoelectric effects without reaching the melting temperature by the lattice, but, nevertheless, with reaching metallic properties.

ACKNOWLEDGMENTS

This study was supported by the Russian Science Foundation (project no. 15-11-00032) and the Competitiveness Enhancement Program of the MEPhI.

REFERENCES

1. A. A. Ionin, S. I. Kudryashov, L. V. Seleznev, et al., Zh. Eksp. Teor. Fiz. **116**, 347 (2013).
2. D. W. Bäuerle, *Laser Processing and Chemistry* (Springer-Verlag, Berlin, 2000).
3. S. A. Akhmanov, N. I. Koroteev, and I. L. Shumay, *Laser Science and Technology* (Harwood Academic, Chur, 1989), Vol. 2.
4. K. Sokolowski-Tinten and D. Von der Linde, Phys. Rev. B **61**, 2643 (2000).
5. *Physical Encyclopedia*, Ed. by A.M. Prokhorov (Soviet Encyclopedia, Moscow, 1990), Vol. 2, p. 37 [in Russian].
6. R. P. Mertens, R. J. Van Overstraeten, and H.J. de Man, Adv. Electron. Electron Phys. **55**, 77 (1981).
7. N. W. Ashcroft and N. D. Mermin, *Solid State Physics* (W. B. Saunders Co., Philadelphia, 1976).
8. O. N. Koroleva, A. V. Mazhukin, V. I. Mazhukin, and P. V. Breslavskiy, Mathematica Montisnigri **35**, 37 (2016).
9. O. N. Koroleva, A. V. Mazhukin, V. I. Mazhukin, and P. V. Breslavskiy, Mathematical Models and Computer Simulations **9**, 383 (2017).
10. Henry M. van Driel, Phys. Rev. B **35**, 8166 (1987).
11. Y. P. Varshni, Physica **34**, 149 (1967).
12. R. J. Van Overstraeten and R. P. Mertens, Solid-State Electron. **30**, 1077 (1987).
13. S. C. Jain, J. M. McGregor, and D. J. Roulston, J. Appl. Phys. **68**, 3747 (1990).
14. G. Borghs, K. Bhattacharyya, K. Denette, et al., J. Appl. Phys. **66**, 4381 (1989).
15. H. P. D. Schenk, S. I. Borenstain, A. Berezin, et al., J. Appl. Phys. **103**, 103502(1) (2008).
16. V. Alex, S. Finkbeiner, and J. Weber, J. Appl. Phys. **79**, 6943 (1996).